Journal of Alloys and Compounds 785 (2019) 445–451

Contents lists available at ScienceDirect

Journal of Alloys and Compounds

journal homepage: http://www.elsevier.com/locate/jalcom

Thermal conductivity of giant magnetocaloric Mn compounds

Hirofumi Wada [a, *], Kosuke Fukuda [a], Takayuki Ohnishi [b], Kei Soejima [b], Kensuke Otsubo [b], Keiichiro Yamashita [b]

[a] Department of Physics, Kyushu University, Motooka 744, Nishi-ku, Fukuoka 819-0395, Japan
[b] Research & Development Group, Dyden Cooperation, Kamimine-cho, Miyaki-gun, Saga, 849-0124, Japan

ARTICLE INFO

Article history:
Received 25 October 2018
Received in revised form
14 December 2018
Accepted 14 January 2019
Available online 17 January 2019

Keywords:
Thermal conductivity
Magnetocaloric effect
Electrical resistivity
First-order magnetic transition

ABSTRACT

Temperature dependence of the thermal conductivity of $Mn_{1.03}As_{0.70}Sb_{0.30}$ and Ru-doped or Ni-doped $(MnFeRu)_2(PSi)$ was studied. These compounds undergo a first-order magnetic transition (FOMT) near room temperature and exhibit a giant magnetocaloric effect at around the Curie temperature. The thermal conductivity of Ru-doped and Ni-doped compounds is abruptly reduced at the Curie temperature during the first cooling. This is due to the micro-cracks generated during the FOMT. On heating, the thermal conductivity shows positive temperature dependence. The Ru-doped and Ni-doped compounds show small humps in the temperature dependence of the thermal conductivity near T_C. The thermal conductivity of ferromagnetic metals is given by the sum of the phonon component, the electronic component, and the magnetic component. The results are discussed by taking account of the temperature dependence of each component.

1. Introduction

The magnetocaloric effect (MCE) is defined as the changes in temperature and entropy of magnetic materials upon application or removal of a magnetic field. Magnetic refrigeration is a straightforward application of the MCE. This cooling technology is quite attractive, because it is highly energy-efficient and environmentally friendly. Over the last two decades, both the refrigeration system and the magnetic refrigerant materials have been extensively developed. With respect to materials, two types of magnetic refrigerants have been proposed near room temperature. One is Gd metal and its alloys. The pure Gd metal is ferromagnetic with a Curie temperature T_C of 294 K. Due to a large magnetic moment and small magnetocrystalline anisotropy, Gd shows substantial MCEs over a wide range of temperatures centered at T_C. Since the first demonstration of magnetic cooling by Broun in 1976 [1], Gd has been used as a magnetic refrigerant in most of magnetic refrigeration prototypes near room temperature. The other type of magnetic refrigerant is the first-order magnetic transition (FOMT) system. Some ferromagnetic compounds are known to undergo a FOMT near room temperature. In 1997, Pecharsky and Gschneidner, Jr. reported giant MCEs of $Gd_5Si_2Ge_2$, which undergoes the FOMT at $T_C = 276$ K [2]. Since then, giant MCEs have been found for various systems exhibiting the FOMT, such as $Mn_{1+\delta}As_{1-x}Sb_x$ [3], $MnFeP_{1-x}As_x$ [4], $La(Fe_{1-x}Si_x)_{13}$ and its hydride [5,6], and NiMnSn Heusler alloys [7]. In particular, $Mn_{2-x}Fe_xP_{1-y}Si_y$, which is a system derived from $MnFeP_{1-x}As_x$, and $La(Fe_{1-x}Si_x)_{13}H_y$ are believed to be the most promising candidates for magnetic refrigerants near room temperature, because they are nontoxic and inexpensive elements and the materials are stable.

The $Mn_{2-x}Fe_xP_{1-y}Si_y$ system has been intensively studied by Brück's group since 2008 [8–10]. The compounds have a hexagonal Fe_2P-type structure in the wide concentration ranges of $0 \le x \le 1$ and $0.28 \le y \le 0.64$. Brück and his colleagues have found that the compounds at around $x = 0.75$ and $y = 0.50$ show excellent properties as magnetic refrigerants, i.e., a sharp FOMT, large MCE, and small thermal hysteresis. They also reported that doping B at around $x = 1.0$ and $y = 0.33$ improves mechanical stability while retaining a high magnetic refrigeration performance [11,12]. Our group have found that Ru-doped $Mn_{2-x}Fe_xP_{1-y}Si_y$ compounds at around $x = 0.75$ and $y = 0.55$ can be good candidates for magnetic refrigerant materials between 275 K and 315 K [13,14].

Thermal conductivity is an important thermophysical property of the magnetic refrigerant materials, because the materials are exposed to a temperature gradient in the current refrigeration system. Though a few reports have been published on the thermal conductivity of the giant MCE systems [15,16], no data have been reported for $Mn_{2-x}Fe_xP_{1-y}Si_y$ compounds. Apart from the

* Corresponding author.
E-mail address: wada@phys.kyushu-u.ac.jp (H. Wada).

https://doi.org/10.1016/j.jallcom.2019.01.188
0925-8388/

application aspect, we considered that it would be of interest to study the thermal conductivity of the magnetic systems undergoing the FOMT. In this paper, we report the temperature dependences of the thermal conductivity and electrical resistivity of $Mn_{1.03}As_{0.70}Sb_{0.30}$ and Ru-doped or Ni-doped $(MnFeRu)_2(PSi)$, which exhibit a giant MCE near room temperature [14,17,18].

2. Experiments

We synthesized $Mn_{1.03}As_{0.70}Sb_{0.30}$, $Mn_{1.24}Fe_{0.60}Ru_{0.16}P_{0.46}Si_{0.54}$, $Mn_{1.30}Fe_{0.64}Ni_{0.06}P_{0.49}Si_{0.51}$, and $Mn_{1.06}Fe_{0.60}Ru_{0.04}P_{0.45}Si_{0.55}$ by sintering and subsequent annealing. Previously, we revealed that $Mn_{1+\delta}As_{1-x}Sb_x$ undergoes the FOMT from a ferromagnetic to paramagnetic state in the concentration range of $0 \leq x \leq 0.30$ [17]. In this system, Mn is slightly enriched ($\delta \leq 0.03$) to obtain a single phase. The $Mn_{1.03}As_{0.70}Sb_{0.30}$ compound was prepared by using the recipe described in ref. 17. The sample was confirmed to be a single phase with the NiAs-type hexagonal structure by X-ray diffraction. The $Mn_{1.24}Fe_{0.60}Ru_{0.16}P_{0.46}Si_{0.54}$ sample is identical to sample 1 in ref. 14. Details of the sample preparation were described there. Hereafter, this compound is labeled F-$(MnFeRu)_2(PSi)$. The $Mn_{1.30}Fe_{0.64}Ni_{0.06}P_{0.49}Si_{0.51}$ sample, labeled F-$(MnFeNi)_2(PSi)$, was prepared in a manner similar to F-$(MnFeRu)_2(PSi)$. The sintering and annealing were done at 1080 °C. No foreign phase other than the Fe_2P-type hexagonal phase was detected for either the F-$(MnFeRu)_2(PSi)$ or F-$(MnFeNi)_2(PSi)$ samples in the X-ray analyses. We found that the ferromagnetism of Ru-doped $Mn_{2-x}Fe_xP_{1-y}Si_y$ was easily collapsed by Ru over-doping or off-stoichiometry. To study the transport properties of non-ferromagnetic compounds, we prepared $Mn_{1.06}Fe_{0.60}Ru_{0.04}P_{0.45}Si_{0.55}$, in which the transition metals were deficient, with a ratio of (MnFeRu): (PSi) = 1.7:1. The compound was labeled NM-$(MnFeRu)_2(PSi)$. The X-ray diffraction pattern of the NM-$(MnFeRu)_2(PSi)$ sample revealed the coexistence of a main phase with the Fe_2P-type structure and the impurity phases with unknown structures.

The temperature dependence of magnetization M was measured in a commercial superconducting quantum interference device magnetometer (Quantum Design MPMS). The samples were first cooled down to the lowest temperature in zero magnetic field before measurements. Then, the M - T curve was measured on heating. For the FOMT systems, the M - T curve on cooling was measured subsequently. Electrical resistivity measurements were carried out by a standard four-probe technique using an a.c. resistance bridge. Thermal conductivity was measured by a steady-state method using a home-made apparatus. The sample has a rectangular shape with typical dimensions of $2 \times 2 \times 10$ mm^3. One end of the sample is mechanically connected to a heat reservoir and a small heater (strain gauge) is attached to the other end. The steady-state heat flow Q generated by joule heating of a heater gives the temperature gradient through the sample. By measuring the temperature difference ΔT between two points of the sample along the heat flow, the thermal conductivity λ was obtained from the following equation:

$$\lambda = \frac{Qd}{S\Delta T}, \quad (1)$$

where d is the distance between the two points and S is the cross-sectional area of the sample. The type E (Chromel-Constantan) differential thermocouple with 0.05 mm diameter was used for ΔT measurements. The temperature dependence of λ can be measured from 4.2 K to room temperature on heating. The measurements from room temperature to 150 K on cooling are also possible. To check the apparatus, we measured the $\lambda - T$ curves of pure Ti (4.2 K-300 K) and pure Gd (100 K-300 K). The results are in agreement with the $\lambda - T$ curves in the literature within an accuracy of 5% [19].

3. Experimental results

Fig. 1 (a) shows the temperature dependence of the magnetization of all the samples in a magnetic field of 1 T. The compounds of $Mn_{1.03}As_{0.70}Sb_{0.30}$, F-$(MnFeRu)_2(PSi)$ and F-$(MnFeNi)_2(PSi)$ show ferromagnetic behavior. The sharp changes in the M - T curves of these compounds near T_C suggest the FOMT. The M - T curves of $Mn_{1.03}As_{0.70}Sb_{0.30}$ are accompanied by thermal hysteresis of about 2 K. No clear hysteretic behavior was observed for F-$(MnFeRu)_2(PSi)$ and F-$(MnFeNi)_2(PSi)$. The Curie temperatures of $Mn_{1.03}As_{0.70}Sb_{0.30}$, F-$(MnFeRu)_2(PSi)$ and F-$(MnFeNi)_2(PSi)$, determined from the M - T curves at 1 T on heating, are 245, 283, and 237 K, respectively. In contrast, no ferromagnetic component was observed for NM-$(MnFeRu)_2(PSi)$. The temperature dependence of the magnetic susceptibility χ of this compound between 2 and 300 K is displayed in Fig. 1 (b). The χ - T curve has a maximum at around 65 K, suggesting antiferromagnetic or spin glass behavior of NM-$(MnFeRu)_2(PSi)$ at low temperatures.

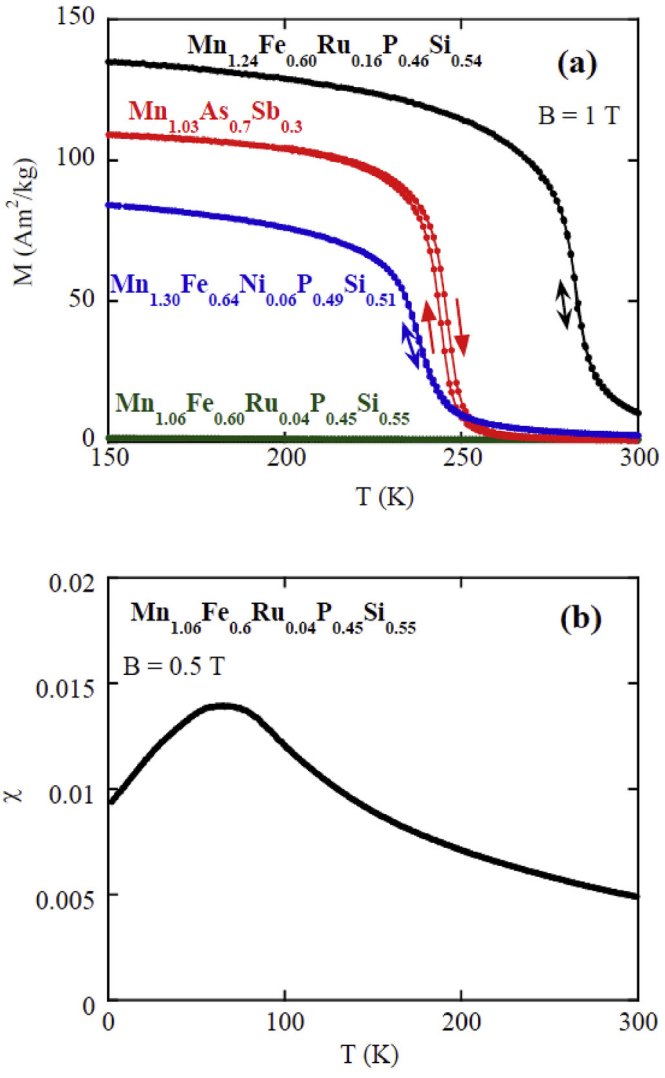

Fig. 1. (a) Temperature dependence of the magnetization M of $Mn_{1.03}As_{0.70}Sb_{0.30}$, $Mn_{1.24}Fe_{0.60}Ru_{0.16}P_{0.46}Si_{0.54}$, $Mn_{1.30}Fe_{0.64}Ni_{0.06}P_{0.49}Si_{0.51}$, and $Mn_{1.06}Fe_{0.60}Ru_{0.04}P_{0.45}Si_{0.55}$ in a magnetic field of 1 T. (b) Temperature dependence of the magnetic susceptibility χ of $Mn_{1.06}Fe_{0.60}Ru_{0.04}P_{0.45}Si_{0.55}$.

The temperature dependence of the electrical resistivity ρ of $Mn_{1.03}As_{0.70}Sb_{0.30}$ is depicted in Fig. 2. The $Mn_{1.03}As_{0.70}Sb_{0.30}$ compound is metallic and it has a large resistivity of about 12 μΩm at room temperature. Haneda et al. measured the $\rho - T$ curves of MnAs single crystals and found anisotropic behavior of resistivity [20]. They reported $\rho_c < \rho_{ab}$, where ρ_c and ρ_{ab} are the resistivities measured with the current flow along and perpendicular to the *c*-axis, respectively. Just above T_C of 318 K, ρ_c and ρ_{ab} are 3.7 and 34 μΩm, respectively. Our data on the polycrystalline $Mn_{1.03}As_{0.70}Sb_{0.30}$ at room temperature are of the same order of magnitude as the latter value. The ρ of $Mn_{1.03}As_{0.70}Sb_{0.30}$ rapidly increases with increasing temperature at around 240 K, reflecting a ferromagnetic to paramagnetic transition. Similar behavior was also reported for MnAs [20].

Fig. 3 illustrates the $\lambda - T$ curve of $Mn_{1.03}As_{0.70}Sb_{0.30}$ between 100 and 298 K. The measurements were carried out on heating. The thermal conductivity increases with increasing temperature in this temperature range. The absolute value of λ at 295 K is 3.0 W/m K at room temperature, which is one order of magnitude smaller than that of typical metallic compounds. Fujieda et al. reported the temperature dependence of thermal conductivity of MnAs [15]. Our $\lambda - T$ curve of $Mn_{1.03}As_{0.70}Sb_{0.30}$ resembles to that of MnAs both qualitatively and quantitatively. The $\lambda - T$ curve changes the slope at around T_C and λ increases more rapidly with temperature above T_C. The thermal conductivity of metallic ferromagnets can be expressed by the sum of the phonon component λ_p, the electronic component λ_e, and the magnetic component λ_m as

$$\lambda = \lambda_p + \lambda_e + \lambda_m. \quad (2)$$

The electronic component can be estimated from the Wiedemann-Franz law as

$$\lambda_e = \frac{LT}{\rho}, \quad (3)$$

where L is the Lorenz number, $L = 2.44 \times 10^{-8}\,W\Omega/K^2$. Assuming that the Wiedemann-Franz law holds for the present system, we estimated λ_e using the resistivity data above 150 K, which is shown in Fig. 3 by the blue symbols. As expected from the large ρ values, the λ_e of $Mn_{1.03}As_{0.70}Sb_{0.30}$ is small. It is found that λ_e gradually increases with increasing temperature above T_C. Therefore, the steep slope of the $\lambda - T$ curve in the paramagnetic state originates in the phonon component, because λ_m does not contribute to λ above T_C.

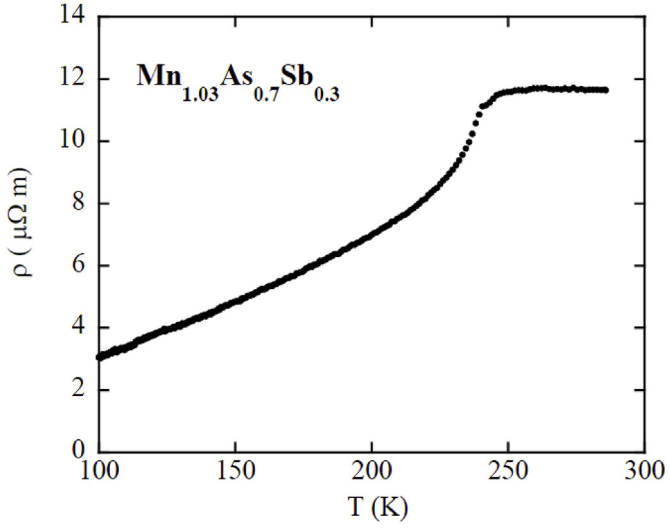

Fig. 2. Temperature dependence of the electrical resistivity ρ of $Mn_{1.03}As_{0.70}Sb_{0.30}$. The measurements have been done on heating.

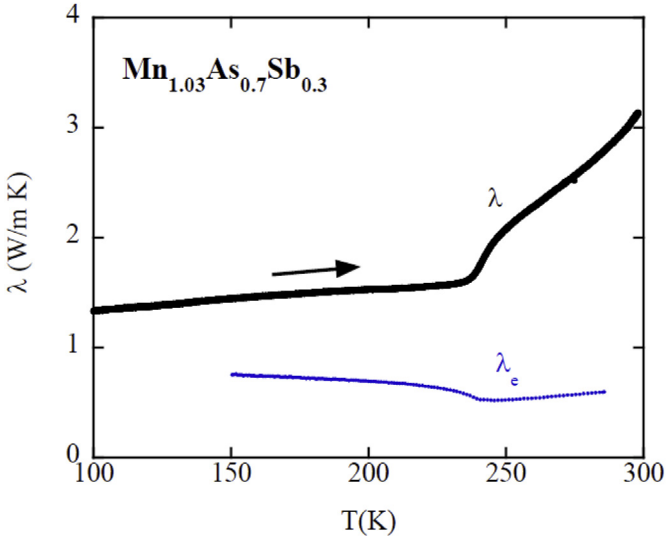

Fig. 3. Temperature dependence of the thermal conductivity λ of $Mn_{1.03}As_{0.70}Sb_{0.30}$. The blue symbols represent the electronic component λ_e estimated from the Wiedemann-Frantz law. (For interpretation of the references to colour in this figure legend, the reader is referred to the Web version of this article.)

The temperature dependence of the electrical resistivity of F-$(MnFeRu)_2(PSi)$ is shown in Fig. 4 (a). The measurements were carried out initially on cooling from room temperature to 4.2 K and subsequently on heating from 4.2 K to room temperature. The initial value of ρ at room temperature is 3.6 μΩm. The resistivity shows a jump at $T_C = 268$ K on cooling, which is clearly lower than the T_C of 281 K on heating. This is "the virgin effect". It has been reported that the Curie temperature of $Mn_{2-x}Fe_xP_{1-y}Si_y$ measured during the first cooling is much lower than that measured in the subsequent cycles [8,21,22]. Therefore, the magnetization vs. temperature curves during the first cycle show very large thermal hysteresis. Unexpectedly, the resistivity dramatically increases with lowering of the temperature below T_C, and finally it reaches 47 μΩm at 4.2 K. On heating, however, the compound shows metallic behavior. The anomalous increase in ρ on cooling originates in the micro-cracks introduced during the FOMT, as pointed out by Guillou et al. [12]. The generation of micro-cracks was directly confirmed by microscopic observations [21,22]. The FOMT of $Mn_{2-x}Fe_xP_{1-y}Si_y$ is accompanied by discontinuous jumps of the lattice parameters: *a* expands, while *c* shrinks just below T_C [10]. These anisotropic changes in the lattice parameters generate micro-cracks at the transition. Moreover, *a* is increased and *c* is decreased gradually with lowering temperature, which make the micro-cracks grow, resulting in a large increase in ρ on cooling. The $\rho - T$ curve on heating shows a small jump at T_C. This fact suggests that fewer micro-cracks were generated on heating. The resistivity decreases with increasing temperature above T_C. Guillou et al. observed similar behavior for B-substituted $Mn_{2-x}Fe_xP_{1-y}Si_y$ [12] but its reason is unclear.

The $\rho - T$ curves of F-$(MnFeRu)_2(PSi)$ during the first three cycles between 250 K and 300 K are depicted in Fig. 4 (b). The compound shows the largest change in ρ during the first cooling and the resistivity at room temperature continuously grows with each cycle. In this temperature range, the resistivity decreases with increasing temperature on both heating and cooling after the first cooling. Guillou et al. reported that the B substitution for $Mn_{2-x}Fe_xP_{1-y}Si_y$

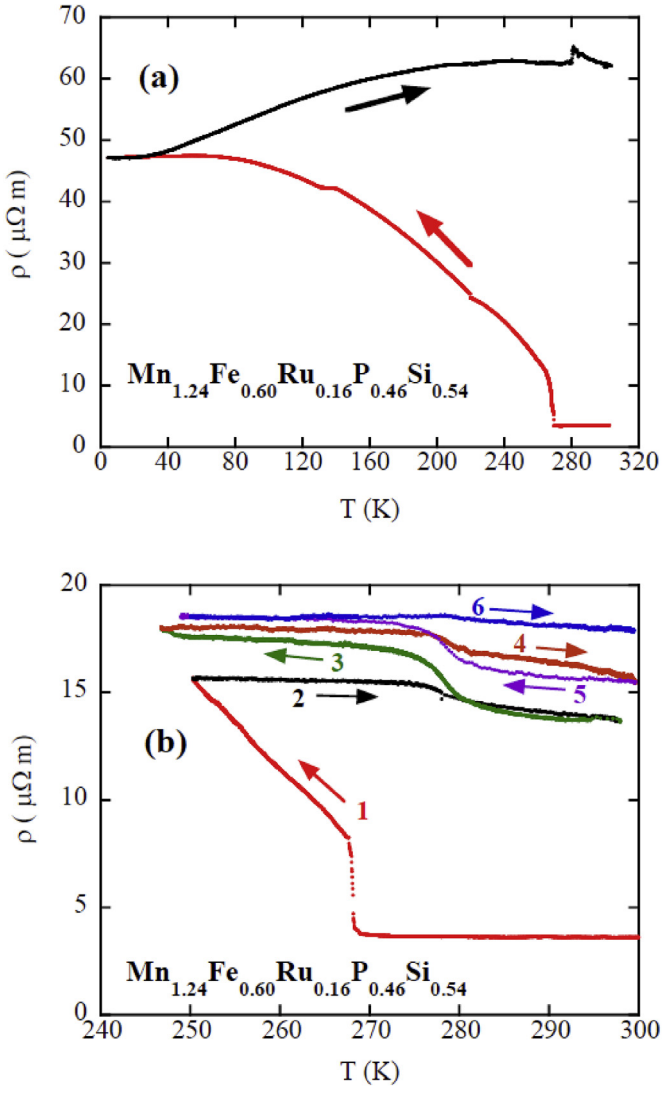

Fig. 4. (a) Temperature dependence of the electrical resistivity of $Mn_{1.24}Fe_{0.60}Ru_{0.16}P_{0.46}Si_{0.54}$, (F-(MnFeRu)$_2$(PSi)). The measurements were carried out first on cooling from room temperature to 4.2 K and then on heating from 4.2 K to room temperature. (b) The $\rho - T$ curves of F-(MnFeRu)$_2$(PSi) during the first three cycles between 250 K and 300 K.

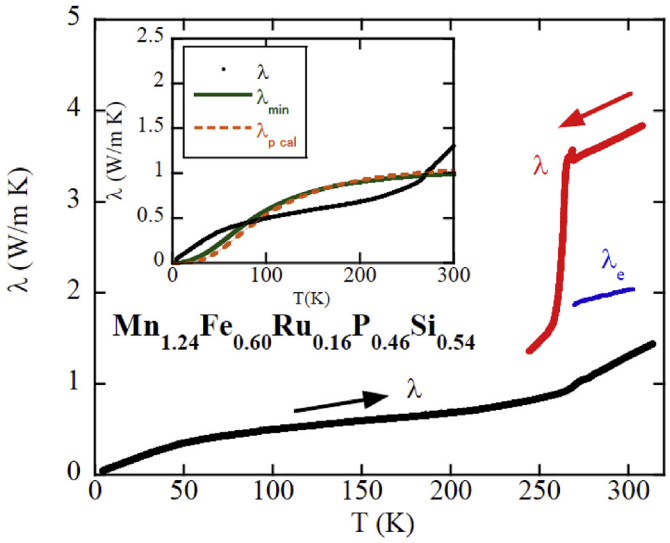

Fig. 5. Temperature dependence of the thermal conductivity of F-(MnFeRu)$_2$(PSi). The $\lambda - T$ curve was initially measured on cooling and was subsequently measured on heating. The blue symbols represent the λ_e above T_C on the first cooling, which were estimated from the Wiedemann-Frantz law. The inset shows the calculated minimum thermal conductivity λ_{min} and the calculated phonon component $\lambda_{p\ cal}$ under the assumption of a constant l_p, as functions of temperature, together with the $\lambda - T$ curve on heating (see text). (For interpretation of the references to colour in this figure legend, the reader is referred to the Web version of this article.)

improves the mechanical stability remarkably [11,12]. They measured the $\rho - T$ curves of the B-substituted and B-free $Mn_{2-x}Fe_xP_{1-y}Si_y$ compounds between 200 and 340 K. According to their results, the ρ values of the B-substituted compound at room temperature after several cycles are in the range of 12–16 μΩm, which is one or two orders of magnitude smaller than those of the B-free compounds. We point out that the ρ values of F-(MnFeRu)$_2$(PSi) at room temperature after three cycles are comparable to those of B-substituted compounds. This fact suggests good mechanical stability of F-(MnFeRu)$_2$(PSi).

The temperature dependence of thermal conductivity of F-(MnFeRu)$_2$(PSi) is displayed in Fig. 5. First, we measured the $\lambda - T$ curve on cooling from room temperature to 240 K. Then, the sample was cooled down to 4.2 K and the $\lambda - T$ curve was measured on heating from 4.2 K to room temperature. The initial value of λ at 300 K is 3.8 W/m K, which is comparable to that of $Mn_{1.03}As_{0.70}Sb_{0.30}$. With decreasing temperature, λ first decreases linearly and then is abruptly reduced by more than half at around 263 K. The remarkable reduction in λ is attributable to the micro-cracks introduced during the FOMT. On the other hand, λ increases smoothly with increasing temperature from 4.2 K to room temperature. The $\lambda - T$ curve changes the slope at around T_C of 280 K. The λ value at 300 K after heating is 1.3 W/m K, which is about one third of the initial value. We consider the electronic contribution to λ of F-(MnFeRu)$_2$(PSi). Once the sample is cooled below T_C, the resistivity becomes anomalously large. This suggests that the Wiedemann-Franz law is not applicable below T_C, because the mean free path of electrons, l_e, does not satisfy the Ioffe and Regel criterion for metallic conduction, $d_0 < l_e$, where d_0 is the interatomic distance. However, we can estimate λ_e for the $\rho - T$ curve on the first cooling above T_C, because the micro-cracks were not generated at this stage. Using the $\rho - T$ data during the first cooling in Fig. 4 (a), we calculated λ_e from Eq. (3) between 270 and 300 K, which is shown in Fig. 5 by the blue symbols. The λ_e at 300 K is evaluated as 2.0 W/m K. We expect that the electronic contribution to λ during heating is quite small, though the Wiedemann-Franz law is not applicable. These results indicate that λ in the paramagnetic state during heating mainly originates in the phonon component, because the magnetic component does not persist above T_C. Before the initial cooling, the phonon component can be evaluated from the difference between λ and λ_e. The above values give $\lambda_p = 1.8$ W/m K at 300 K. It should be noted that λ at 300 K after heating (1.3 W/m K) is smaller than this λ_p. This means that the phonon component is also reduced during the FOMT. Detailed discussion on this point will be given later.

To investigate the effects of the thermal cycle on thermal conductivity, we measured the $\lambda - T$ curves of F-(MnFeRu)$_2$(PSi) during the first four heating processes, which are illustrated in Fig. 6. In contrast to the $\rho - T$ curves in Fig. 4 (b), the $\lambda - T$ curve is not sensitive to the thermal cycle after the first cooling. We emphasize that the reproducibility of the temperature dependence of bulk transport property demonstrates good mechanical stability of the F-(MnFeRu)$_2$(PSi) compound, once the sample is cooled below T_C. The $\lambda - T$ curve on the first heating has a small hump near T_C. The hump height is dependent on the thermal cycle. Even on the fourth

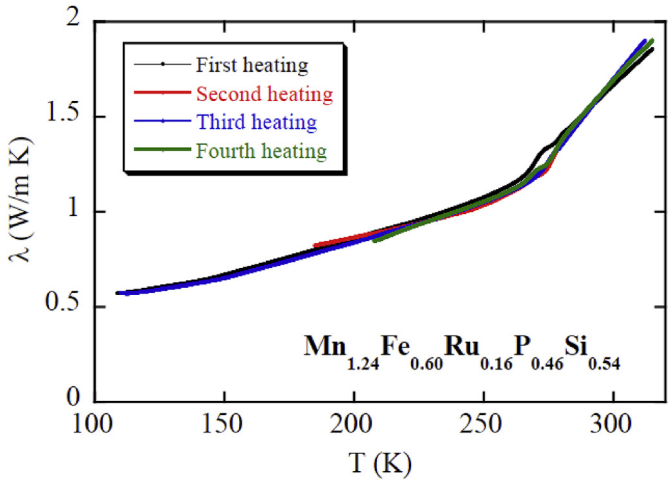

Fig. 6. The $\lambda - T$ curves of F-$(MnFeRu)_2(PSi)$ during the first four heating processes.

heating, a tiny hump was detected. The origin of the hump in the $\lambda - T$ curve will be discussed later.

The temperature dependences of the thermal conductivity of F-$(MnFeNi)_2(PSi)$ and NM-$(MnFeRu)_2(PSi)$ are shown in Fig. 7. For F-$(MnFeNi)_2(PSi)$, the $\lambda - T$ curve on the first cooling and that on the subsequent heating are depicted. The electronic contribution to λ_e, which was estimated for the initial cooling process between room temperature and T_C, is also plotted by the blue symbols. The $\lambda - T$ curves of F-$(MnFeNi)_2(PSi)$ are quite similar to those of F-$(MnFeRu)_2(PSi)$. The thermal conductivity is remarkably reduced at T_C during the first cooling, while it increases continuously on heating. The slope of the $\lambda - T$ curve becomes steep above T_C. The λ values at 295 K before and after cooling are 3.8 and 1.3 W/m K, respectively.

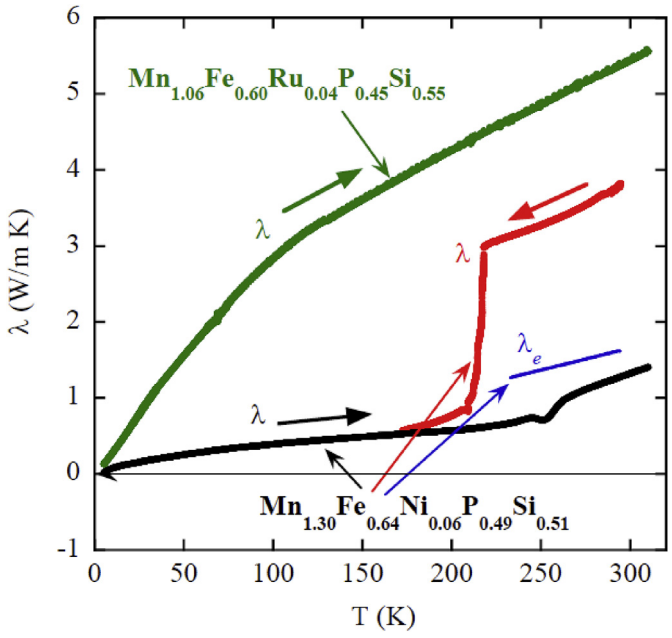

Fig. 7. Temperature dependence of the thermal conductivity of $Mn_{1.30}Fe_{0.64}Ni_{0.06}P_{0.49}Si_{0.51}$ (F-$(MnFeNi)_2(PSi)$) and $Mn_{1.06}Fe_{0.60}Ru_{0.04}P_{0.45}Si_{0.55}$ (NM-$(MnFeRu)_2$(-PSi)). The measurement sequence of the $\lambda - T$ curve of F-$(MnFeNi)_2(PSi)$ is the same as that of F-$(MnFeRu)_2(PSi)$. The $\lambda - T$ curve of NM-$(MnFeRu)_2(PSi)$ was measured on heating. The blue symbols represent the λ_e of F-$(MnFeNi)_2(PSi)$ above T_C on the first cooling. (For interpretation of the references to colour in this figure legend, the reader is referred to the Web version of this article.)

The λ_e at 295 K is evaluated as 1.6 W/m K. The phonon component before cooling is estimated to be 2.2 W/m K at 295 K from the difference between λ and λ_e, which is clearly larger than the λ of 1.3 W/m K at 295 K after cooling. This is similar to the case of F-$(MnFeRu)_2(PSi)$. A small hump was also observed just below T_C in the $\lambda - T$ curve on heating.

The $\lambda - T$ curve of NM-$(MnFeRu)_2(PSi)$ was measured on heating. The thermal conductivity increases rapidly at low temperatures and nearly linearly above 150 K with increasing temperature. The λ value at 295 K is 5.4 W/m K, which is larger than those of the other three compounds. We measured the $\rho - T$ curve of NM-$(MnFeRu)_2(PSi)$. The electrical resistivity of the compound is nearly independent of temperature between 10 K and room temperature with a value of 4 μΩm. This value is comparable to that of F-$(MnFeRu)_2(PSi)$ at room temperature before cooling. Sales et al. prepared $MnFeP_{0.8}Si_{0.2}$ single crystals by a flux method [23]. Their magnetic measurements revealed that this compound is antiferromagnetic with a Néel temperature of 158 K. According to their $\rho - T$ data, the ρ_c value $MnFeP_{0.8}Si_{0.2}$ at room temperature is about 2.5 μΩm. This fact means that the intrinsic ρ of $(MnFe)_2(PSi)$ is substantially large. We have $\lambda_e = 1.7$ W/m K at 295 K from the Wiedemann-Franz law. The phonon component is obtained from the difference between λ and λ_e, which is 3.7 W/m K at 295 K. These observations suggest that the phonon component of NM-$(MnFeRu)_2(PSi)$ is larger than those of F-$(MnFeRu)_2(PSi)$ and F-$(MnFeNi)_2(PSi)$ at room temperature.

4. Discussion

We have found that the thermal conductivity of F-$(MnFeRu)_2$(-PSi) and F-$(MnFeNi)_2(PSi)$ is abruptly decreased at T_C during the first cooling. This is due to the micro-cracks generated during the FOMT. We also observed the following features in the $\lambda - T$ curves of F-$(MnFeRu)_2(PSi)$ and F-$(MnFeNi)_2(PSi)$.

1. On heating, the $\lambda - T$ curves change the slope at T_C. The thermal conductivity increases more rapidly above T_C. This behavior is also observed for $Mn_{1.03}As_{0.70}Sb_{0.30}$.
2. The $\lambda - T$ curves have small humps near T_C.
3. The phonon component of λ after cooling is smaller than that before cooling.

In the following, we discuss these features. From the analogy of the kinetic theory of gases, the thermal conductivity components of solids, λ_p, λ_e, and λ_m, are expressed as

$$\lambda_i = \frac{1}{3} C_i v_i l_i \quad (i = p,\ e,\ m), \tag{4}$$

where C_i is the corresponding specific heat per volume, and v_i and l_i are the velocity and the mean free path of the particle (phonon, electron, or magnon), respectively. We discuss the temperature dependence of each component of λ based on Eq. (4). First, let us consider the case in which a pure metallic system undergoes the FOMT. In the phonon component, C_p means the lattice specific heat, which has a step at T_C in its temperature dependence, reflecting a change in the phonon dispersion (or the Debye temperature) at the FOMT. In addition, C_p is enhanced near T_C, due to the precursor phenomenon or the fluctuation effect of the FOMT. This does not mean a sharp peak of the specific heat due to the latent heat, because the specific heat cannot be defined at the transition temperature of the FOMT. As the temperature approaches T_C, the lattice becomes unstable, which enhances the specific heat. Above T_C, C_p becomes normal so that the lattice specific heat must have a maximum near T_C. On the other hand, the mean free path of

phonons decreases with increasing temperature following $l_p \propto 1/T$ at high temperatures. Since the sound velocity does not show a significant temperature variation, we expect that λ_p has a maximum near T_C from Eq. (4). For C_e, we only consider the electronic specific heat, which varies linearly with temperature. The temperature dependence of C_e also shows a step at T_C, because the electronic specific heat coefficient suddenly changes at the transition temperature due to the FOMT. The mean free path of electrons decreases with increasing temperature. Like l_p, l_e shows T^{-1} dependence at high temperatures. The Fermi velocity does not change with temperature. As a result, λ_e is nearly independent of temperature at high temperatures, which is often observed for typical metals [19]. The magnetic component mainly arises from the spin wave excitations. At low temperatures, C_m is proportional to $T^{3/2}$. Near T_C, C_m is enhanced due to the magnetic instability, which is similar to C_p. Since C_m vanishes above T_C, the magnetic specific heat has a maximum near T_C. The mean free path of magnon is expected to decrease with increasing temperature. Above T_C, l_m becomes zero. If the magnon velocity is not sensitive to temperature, it is expected that λ_m also has a maximum near T_C and suddenly vanishes above T_C. Sechovský and his coworkers reported the temperature dependence of the thermal conductivity of $ErCo_2$ and $HoCo_2$, which undergo the FOMT from a ferrimagnetic to a paramagnetic state at $T_C = 32$ and 77 K, respectively [24,25]. In these compounds, λ shows a positive jump at T_C with decreasing temperature and the $\lambda - T$ curve has a broad maximum below T_C. We point out that these characteristics can be accounted for by the above scenario on the temperature dependences of λ_p and λ_m. For the present $(MnFe)_2(PSi)$ compounds, however, the situation is somewhat different. The FOMT of the Mn compounds is realized not in the pure system but in the alloyed system. When the FOMT takes place in the alloyed system, the high-temperature phase and the low-temperature phase coexist in a certain temperature range near T_C. The coexistence of the two phases in the $(MnFe)_2(PSi)$ compounds has been confirmed by diffraction studies by several groups [10,26,27]. This may have strong impacts on l_p and l_m. In general, the two-phase region comprises the microstructures. Therefore, we expect that l_p and l_m are considerably reduced in the two-phase region. This suggests that the mean free path of phonons shows a minimum near T_C in the temperature dependence. On the other hand, l_m rapidly decreases near T_C and vanishes above T_C. Moreover, alloying generally destroys a sharp FOMT by rounding, which suppresses the peaks of C_p and C_m. Therefore, the peak of λ diminishes or disappears in some cases. The small humps of the $\lambda - T$ curves of F-$(MnFeRu)_2(PSi)$ and F-$(MnFeNi)_2(PSi)$ can be understood in this scenario. Sechovský et al. measured the $\lambda - T$ curves of $Ho(Co_{0.95}Si_{0.05})_2$ and $Er(Co_{0.95}Si_{0.05})_2$ [24,25]. They found that the substitution of 5% Si for Co reduces the peak of λ seriously, though the compounds still undergo the FOMT. Our explanation is also applicable to these observations. To validate our interpretation, detailed X-ray diffraction measurements on the two-phase region near T_C are strongly desired.

In the ferromagnetic $(MnFe)_2(PSi)$ compounds, the first cooling generates micro-cracks, which has strong effects on l_p and l_e. The huge electrical resistivity of F-$(MnFeRu)_2(PSi)$ after the initial cooling suggest that the Drude-Lorentz model for DC conductivity is no longer valid. Though we cannot evaluate λ_e from the Wiedemann-Franz law, the small λ values indicate that the electronic component makes little contribution to the thermal conductivity on heating. In the case of the phonon component, l_p is related to the relaxation rate $1/\tau_p$ as $1/\tau_p = v_p/l_p$. It is known that $1/\tau_p$ follows the Matthiessen's rule, $1/\tau_p = \sum 1/\tau_i$, where $1/\tau_i$ represents the relaxation rate of individual scattering mechanisms, such as grain boundary scattering, umklapp scattering, and lattice defect scattering, etc. Before the initial cooling, various mechanisms contribute to $1/\tau_p$. Once the sample is cooled, a number of micro-cracks are generated, and these become new scattering sources of phonons. This increases the relaxation rate and hence makes l_p smaller. Therefore, λ_p is reduced after cooling.

Finally, we discuss a change in the slope of the $\lambda - T$ curves on heating at T_C. Since the electronic component is quite small, λ is expressed as the sum of the phonon component and the magnetic component in the ferromagnetic state on heating. The gentle slope of the $\lambda - T$ curve in the ferromagnetic state near T_C is a consequence of the damped peaks of λ_p and λ_m due to alloying. On the other hand, the phonon component plays a dominant role in λ above T_C on heating, so that λ_p is responsible for a steep slope in the $\lambda - T$ curve above T_C. This is also demonstrated by the facts that the slope of the $\lambda - T$ curve in the paramagnetic state before the first cooling is at the same level as that on heating, while λ_e is weakly dependent on temperature. Next, we consider the origin of the positive temperature dependence of λ_p. Usually, λ_p of crystalline materials decreases with increasing temperature at high temperatures. This is because most of the scattering mechanisms for phonons give negative temperature dependence of the relaxation rate. The positive temperature dependence of λ_p at high temperatures has often been reported for glasses, and amorphous and disordered materials. Nearly 70 years ago, Kittel explained the positive temperature dependence of λ_p by assuming a temperature independent l_p in glasses [28]. If l_p is constant, λ_p is proportional to C_p from Eq. (4). Since C_p increases with increasing temperature, λ_p is expected to show a positive temperature dependence. In the present system, l_p originating in micro-cracks is nearly independent of temperature in the first approximation. On the other hand, Cahill and Pohl proposed a model in which thermal conductivity is described as a random walk of the thermal energy between neighboring atoms vibrating with random phases [29]. They have shown that the minimum thermal conductivity due to phonons is expressed as

$$\lambda_{\min} = \left(\frac{\pi}{6}\right)^{1/3} k_B n^{2/3} \sum_j v_j \left(\frac{T}{\Theta_j}\right)^2 \int_0^{\Theta_j/T} \frac{x^3 e^x}{(e^x - 1)^2} dx, \quad (5)$$

where k_B is the Boltzmann constant, n is the atom density per unit volume, and v_j is the sound velocity for each direction of the displacement j (one longitudinal and two transverse modes). Θ_j is the cutoff frequency for each direction expressed in degree, $\Theta_j = v_j(\hbar/k_B)(6\pi^2 n)^{2/3}$, where $\hbar$ is the reduced Planck constant.

In the following, we calculate $\lambda_{\min}$. For simplicity, we assume that the sound velocity of the longitudinal mode equals that of the transverse mode. In this case, Θ_j represents the Debye temperature Θ_D, which can be estimated from the specific heat curve. We reanalyzed the specific heat curve of $Mn_{1.2}Fe_{0.7}Ru_{0.1}P_{0.5}Si_{0.5}$, which was reported by our group previously [13], and obtained $\Theta_D = 420$ K. This value is slightly larger than that of 360 K reported for $MnFeP_{0.8}Si_{0.2}$ by Sales et al. [23]. The sound velocity is calculated from the above equation, and we have $v_p = 3.34 \times 10^3$ m/s. From the values of the lattice parameters, n is obtained as $n = 8.18 \times 10^{28}/m^3$. Putting these values into Eq. (5), the temperature dependence of $\lambda_{\min}$ is obtained, as shown by the solid (green) line in the inset of Fig. 5. The experimental data of λ on heating are also plotted in this figure. It is found that the calculated $\lambda_{\min}$ values are of the same order of magnitude as the experimental values. Although the $\lambda_{\min}$ shows positive temperature dependence up to room temperature, the slope of the $\lambda_{\min} - T$ curve is much gentler at around 300 K. We also calculated the phonon component λ_p from Eq. (4) and the Debye specific heat with $\Theta_D = 420$ K by assuming that l_p is constant.

The temperature dependence of the calculated phonon component $\lambda_{p\ cal}$ with $l_p = 3$ Å is shown by the dashed (orange) line in the inset of Fig. 5, which is nearly the same as the $\lambda_{min} - T$ curve. The adopted l_p value is in the range of typical values for glasses [28]. From these results, we conclude that both the minimum thermal conductivity and Kittel's scenario fail to describe the steep slope of the $\lambda - T$ curves of $(MnFe)_2PSi$. At this moment, the origin of the rapid rise in λ above T_C is not clarified. For further discussion, a comparison with more realistic models is necessary. Calculations of the phonon thermal conductivity from first principles for $(MnFe)_2(PSi)$ are strongly desired.

5. Conclusions

We have studied the thermal conductivity of Mn-based compounds which exhibit giant MCEs near room temperature. The initial λ values of the ferromagnetic Mn compounds at room temperature are 3–4 W/m K. The thermal conductivity of F-$(MnFeRu)_2(PSi)$ and F-$(MnFeNi)_2(PSi)$ is abruptly reduced on the first cooling due to the micro-cracks generated during the FOMT. On heating, λ smoothly increases with increasing temperature. The $\lambda - T$ curves of F-$(MnFeRu)_2(PSi)$ and F-$(MnFeNi)_2(PSi)$ have small humps near T_C. Above T_C, the thermal conductivity increases more rapidly. The electronic component λ_e was estimated from the Wiedemann-Franz law. The characteristics of the $\lambda - T$ curves are discussed in terms of the temperature dependences of the phonon component λ_p and the magnetic component λ_m. We have proposed that the coexistence of a two-phase region by alloying is responsible for the humps in the $\lambda - T$ curve. We found that the thermal cycle has little impact on the $\lambda - T$ curve of F-$(MnFeRu)_2(PSi)$, once the sample is cooled. This suggest the good mechanical stability of the compound.

The thermal conductivity of the Mn-based compounds is low. At room temperature, the λ values of the compounds are 1/5–1/3 of those of Gd and $La(Fe_{1-x}Si_x)_{13}H_y$. Recent magnetic refrigeration prototypes are based on the active magnetic regenerator (AMR). Nielsen and Engelbrecht discussed the effect of λ on the performance of AMR using a numerical model [30]. They showed that the performance may decrease considerably for λ less than 5 W/m K, when the AMR system is operated at a frequency higher than 2 Hz. To improve the thermal conductivity, further developments of materials and/or materials processing are necessary. On the other hand, the dynamic response of magnetocaloric materials to the magnetic field also gives information on the thermal conductivity. Porcari et al. measured the adiabatic temperature change of magnetic materials by an extraction method and estimated the time constant [31]. According to their results, the time constant of temperature change of $(MnFe)_2(PSi)$ is comparable to that of Gd. These facts encourage us to utilize Mn-based compounds as magnetic refrigerant materials near room temperature.

Acknowledgments

We express our gratitude to Dr. Masakazu Ito, Kagoshima University, for his technical advice on the measurements of thermal conductivity. This work was partially supported by JSPS KAKENHI Grant Number 16K04932 and by the Advanced Low Carbon Technology Research and Development Program (ALCA) of the Japan Science and Technology Agency (JST) JPMJAL1408.

References

[1] G.V. Brown, J. Appl. Phys. 47 (1976) 3673.
[2] V.K. Pecharsky, K.A. Gschneidner Jr., Phys. Rev. Lett. 78 (1997) 4494.
[3] H. Wada, Y. Tanabe, Appl. Phys. Lett. 79 (2001) 3302.
[4] O. Tegus, E. Brück, K.H.J. Buschow, F.R. de Boer, Nature 415 (2002) 150.
[5] F.-X. Hu, B.-G. Shen, J.-R. Sun, G.-J. Wang, Z.-H. Cheng, Appl. Phys. Lett. 80 (2002) 826.
[6] A. Fujita, S. Fujieda, Y. Hasegawa, K. Fukamichi, Phys. Rev. B 67 (2003) 104416.
[7] T. Krenke, E. Duman, M. Acet, E.F. Wassermann, X. Moya, L. Manosa, A. Planes, Nat. Mater. 4 (2005) 450.
[8] D.T. Cam Thanh, E. Brück, N.T. Trung, J.C.P. Klaasse, K.H.J. Buschow, Z.Q. Ou, O. Tegus, L. Caron, J. Appl. Phys. 103 (2008), 07B318.
[9] N.H. Dung, L. Zhang, Z.Q. Ou, E. Brück, Appl. Phys. Lett. 99 (2011), 092511.
[10] N.H. Dung, L. Zhang, Z.Q. Ou, E. Brück, Scr. Mater. 67 (2012) 975.
[11] F. Guillou, G. Porcari, H. Yibole, N.H. van Dijk, E. Brück, Adv. Mater. 26 (2014) 2671.
[12] F. Guillou, H. Yibole, N.H. van Dijk, L. Zhang, V. Hardy, E. Brück, J. Alloys Compd. 617 (2014) 569.
[13] H. Wada, K. Nakamura, K. Katagiri, T. Ohnishi, K. Yamashita, A. Matsushita, Jpn. J. Appl. Phys. 53 (2014), 063001.
[14] T. Ohnishi, K. Soejima, K. Yamashita, H. Wada, Magnetochemistry 3 (2017) 6.
[15] S. Fujieda, Y. Hasegawa, A. Fujita, K. Fukamichi, J. Appl. Phys. 95 (2004) 2429.
[16] Y. Shao, M. Zhang, H. Luo, A. Yan, J. Liu, Appl. Phys. Lett. 107 (2015) 152403.
[17] H. Wada, T. Asano, J. Magn. Magn. Mater. 290–291 (2005) 703.
[18] E. Brück, N.T. Trung, Z.Q. Ou, K.H.J. Buschow, Scr. Mater. 67 (2012) 590.
[19] C.Y. Ho, R.W. Powell, P.E. Liley, J. Phys. Chem. Ref. Data 1 (1972) 279.
[20] S. Haneda, N. Kazama, Y. Yamaguchi, H. Watanabe, J. Phys. Soc. Jpn. 42 (1977) 1201.
[21] A. Bartok, M. Kustov, L.F. Cohen, A. Pasko, K. Zehani, L. Bessais, F. Mazaleyrat, M. LoBue, J. Magn. Magn. Mater. 400 (2016) 333.
[22] M. Fries, L. Pfeuffer, E. Bruder, T. Gottschall, S. Ener, L.V.B. Diop, T. Gröb, K.P. Skokov, O. Gutfleisch, Acta Mater. 132 (2017) 222.
[23] B.C. Sales, M.A. Susner, B.S. Conner, J.Q. Yan, A.F. May, Phys. Rev. B 92 (2015) 104429.
[24] D. Vasylyev, J. Prokleška, J. Šebek, V. Sechovský, J. Alloys Compd. 394 (2005) 96.
[25] V. Sechovský, D. Vasylyev, J. Prokleška, Z. Naturforsch. B 62 (2007) 965.
[26] V. Hoglin, M. Hudl, M. Sahlberg, P. Nordblad, P. Beran, Y. Andersson, J. Solid State Chem. 184 (2011) 2434.
[27] N.H. Dung, L. Zhang, Z.Q. Ou, L. Zhao, L. van Eijck, A.M. Mulders, M. Avdeev, E. Suard, N.H. van Dijk, E. Brück, Phys. Rev. B 86 (2012), 045134.
[28] C. Kittel, Phys. Rev. 75 (1949) 972.
[29] D.G. Cahill, S.K. Watson, R.O. Pohl, Phys. Rev. B 46 (1992) 6131.
[30] K.K. Nielsen, K. Engelbrecht, J. Phys. D 45 (2012) 145001.
[31] G. Porcari, K. Morrison, F. Cugini, J.A. Turcaud, F. Guillou, A. Berenov, N.H. van Dijk, E.H. Brück, L.F. Cohen, M. Solzi, Int. J. Refrig. 59 (2015) 29.